Estimation of the power ratio and torque in wind turbine Savonius rotors using artificial neural networks

J. Sargolzaei and A. Kianifar

Abstract— The power factor and torque of wind turbines are estimated using artificial neural networks (ANNs) based on experimental that are collected over seven prototype vertical Savonius rotors. Unlike horizontal-axis turbines, in vertical-axis turbines rotation speed is low and torque is high. Therefore, this device could be used for local production of electricity. In this research, the rotors having different features in the wind tunnel and the tests are repeated 4 to 6 times for reducing error. All experiments are done on six blades in different Reynolds number and wind speed varied from 8 to 14 m/s. Input quantity for the estimation in neural network is tip speed ratio (TSR). Rotor's power factor and torque were simulated in different Reynolds numbers and different angles of blade in proportion to blowing wind in a complete rotation. The simulated Results were compared with the corresponding experimental data shows that the simulation has the capability of providing reasonable estimations for the maximum power of rotors and maximizing the efficiency of Savonius wind turbines. According to results, increasing Reynolds number leads to increase of power ratio and torque. For all examined rotors, maximum and minimum amount of torque happens in angle about 60° and 120°, respectively.

Keywords— Vertical Savonius rotors, Neural networks, Wind tunnel, Power factor, Torque, Tip speed ratio.

I. INTRODUCTION

Wind turbine is used to change wind energy into mechanical energy (such as wind mill and moving weight) and generate electricity. These turbines are classified to two categories horizontal axis and vertical axis. The horizontal axis wind turbines have complicated structures and difficult installation. This turbine is economically valuable only in areas with permanent winds and high speeds. Although rotation speed is very high, torque is low. This turbine often is used to generate electricity. The vertical-axis wind turbines (VAWTs) have simple structure and installation. They are useful in different speed and direction of wind [1,2]. Unlike horizontal axis turbines, in vertical axis turbines rotation speed is low and torque is high [3]. These turbines are independence from wind direction. Because of low speed and

J. Sargolzaei is with the department of chemical engineering, Ferdowsi university of Mashhad, P.O. Box 9177948944, IRAN (corresponding author to provide phone: +98-511-8815100; fax: +98-511-8816840 e-mail: sargolzaei@ um.ac.ir).

A. Kianifar is with the department of Mechanical engineering, Ferdowsi university of Mashhad, P.O. Box 9177948944, IRAN (corresponding author to provide phone: +98-511-8815100; fax: +98-511-8816840 e-mail: kianifar@ um.ac.ir). Manuscript received January 19, 2007; Revised April 4, 2007

high torque in these turbines, some forms of power transfer such as compressed air and hydraulic have preference to generate electricity. This device could be used for pumping water in agriculture and industry [4].

In vertical axis wind turbines or rotors, such as Savonius [5] rotating axis is perpendicular to wind direction. Therefore the surface which is moved by air, after rotating half a round, should move in reverse direction of wind. This is the reason of decreasing of power ratio. Therefore blade is an important factor in these rotors. The Savonius rotor includes two half cylinder shape blades (nominal diameter D, height S), as shown in Fig. 1. The movement is mainly the result of the different between the drag on the advancing paddle and the drag on the other one. The lift force, which normally takes place to the direction of wind velocity, produces the rotation in this type of turbine. There is high pressure before the surface whereas low pressure after it [3].

Kavamora and his colleagues in 2001 studied the flow round Savonius rotor by DDM method (Domain Decomposition Method). They examined torque ratio and power ratio of rotor in different speeds of air blow for semicircle blades [6].

All these results have leaded us to build alternative methods of predicting wind turbine performance that is function of power factor and Reynolds number. One of these methods is artificial neural networks (ANNs). Neural networking involves algorithms under which information is accumulated in programmed objects that are capable of learning through much iteration using simulated or real data [7].

ANNs have been used in renewable energy systems as well as for many other disciplines. Comprehensive reviews of ANN applications in energy systems in general [8] and in renewable energy systems in particular [9] are available.

In this research, ANNS have applied to simulation of rotor's power ratio in different Reynolds numbers and different angles of blade in proportion to blowing wind (in a complete rotation). Then, Results were compared with the corresponding experimental data shows that the simulation has the capability of providing reasonable estimations for the maximum power of rotors and maximizing the efficiency of Savonius wind turbines.

II. THEORY

A neural network is by definition: a system of simple processing elements, called neurons, which are connected to a

network by a set of weights (Fig. 2). The network is determined by the architecture of the network, the magnitude of the weights and the processing element's mode of operation. The neuron is a processing element that takes a number of inputs (p), weights them (w), sums them up, adds a bias (b) and uses the result as the argument for a singular valued function, the transfer function (f), which results in the neurons output (a). The most common networks are constructed by ordering the neurons in layers, letting each neuron in a layer take as input only the outputs of neurons in the previous layer or external inputs. To determine the weight values, a set of examples is needed of the output relation to the inputs. Therefore, a set of data was produced describing the whole operating range of the system. The knowledge of the neural network is encoded in the values of its weights.

The task of determining the weights from these examples is called training and is basically a conventional estimation problem. For this purpose, the back-propagation strategy has become the most frequently, and here, used method which tends to give reasonable answers when presented with inputs that they have never seen. Standard back-propagation is a gradient descent in which the network weights are modified by relation follow:

$$w_{ij}(n+1) = w_{ij}(n) + \eta \cdot \delta_i(n) \cdot x_i(n) \tag{1}$$

Where $w_{ij(n+1)}$ weight of i to j element in (n+1)th step and $w_{ij}(n)$ are as same weight in nth step. $\delta_i(n)$ is local error that evaluated to $e_i(n)$ and n is step size [10] and η is the learning rate that is equal 1. The local error is corresponding of relation follow:

$$e_i(n) = d_i(n) - y_i(n) \tag{2}$$

The term back-propagation refers to the manner in which the gradient is computed for non-linear multiple-layer networks. The typical performance function that is used for training feedforward neural networks is the mean sum of squares of the network errors between the network outputs and the target outputs [11]. In this work the batch gradient decent with momentum algorithm [12] was used as the training function. The momentum algorithm is development state of the gradient decent that weights learning obtained from relation follow:

$$w_{ij}(n+1) = w_{ij}(n) + \eta \cdot \delta_i(n) \cdot x_i(n) + \alpha \cdot (w_{ij}(n) - w_{ij}(n-1)) \tag{3}$$

Where α is the momentum coefficient that between 0.1 to 0.9 values. This and other training functions gave good results in earlier neural network modeling of wind turbine. The performance of the neural network model evaluated with the root mean square error (RMSE) and determination coefficient (R^2) between the modeled output and measures of the training data set that their relations are follow:

$$R^2 = 1 - \frac{\sum_P (x_{obs} - x_{est})^2}{\sum_P (x_{pred} - \bar{x}_{obs})^2} \tag{4}$$

$$RMSE = \sqrt{\frac{\sum_P (x_{obs} - x_{est})^2}{N}} \tag{5}$$

Where x_{obs}, x_{est} are experimental and estimated values, respectively, and N is the number of data.

When the RMSE is at the minimum and R^2 is high, ≥ 0.8, a model can be judged as very good [7]. These methods were occasionally used in neural network model validation [7,11].

III. METHODS AND MATERIALS

A. Calculating power of wind force

Kinetic energy of air is calculated by following equation:

$$P_w = \frac{1}{2}\overset{\circ}{m}V^2 \tag{6}$$

That $\overset{\circ}{m}(kg/s)$ is air mass flow rate and $V(m/s)$ is speed of blowing air. By replacing $\overset{\circ}{m}$ energy equation is changeable to power in surface which is swept by rotor:

$$P_w = \frac{1}{2}\rho v^3 A \tag{7}$$

P_w (watt) is power, $\rho(kg/m^3)$ is air density and $A(\pi R^2)$ is surface which is swept by rotor.

Following equation is useful to calculate power produced by turbine:

$$P_t(\theta) = F(\theta) \cdot v(\theta) = T(\theta)\omega(\theta) \tag{8}$$

θ is angular position of turbine, T is torque of vertical force to blade's surface (force of air pressure), v is speed vector in force point of F, and ω is rotating speed of blade.

The power factor can be defined as the ratio between the power in turbine shaft (P_t) and the wind power (P_w) due to its kinetic energy right before the turbine plane, which yields:

$$C_P = \frac{P_t}{P_w} \tag{9}$$

Product of dot multiply in equation 8 shows that only the factor of the force with the same direction of rotation is effective to produce power. Therefore, blade's curve in vertical axis turbine is very important.

B. Produced Samples

Savonius rotor has been tested with six different blade's curves in a square section wind tunnel to dimension $0.4 \times 0.4 \times 14$ m. In rotors "I" to "V" each blade is a semicircle to the diameter value 16 cm. Values of s distances (gap) are 0, 3.2, 3.8, 6.4, and 7.2 cm for rotors "I" to "VI" in Fig. 3, respectively.

These gap distance change amount of drag force on back and front of blade in different angles in proportion to blowing wind. The blade's curve in rotor "VI" is Savonius curve which is similar to rotor "IV" in dimensions. Height (H) in all produced models is about 30 cm, thickness of blade is 1 mm, and it is made of aluminum. Fig. 3 shows rotors shapes.

C. Experimentation of Different Blades in Wind Tunnel

Blade's power factor is calculated by measuring rotating speed of rotor round axis and outlet torque which is measured by two special dynamometer connected to the end of each blade. All experiments are done in the same situation and wind speed varies from 8 to $14 \, \mathrm{m/s}$. In the first experiment, rotation speed and torque of each rotor are measured in a complete rotation and results are compared with other rotors. In the next phase, same experiment is done on each blade in different Reynolds number (different speeds of wind) and the effect of Reynolds number (wind speed) on rotor's power is examined.

The result of experiments for rotors "I" and "IV" are presented. Results of previous experiments make it possible to calculate and compare average power factor in a complete rotation in a specific wind speed. This comparison could be a good standard to select the rotor with the best efficiency.

Variables tip speed ratio (λ), power factor (Cp) and Reynolds number (Re) are defined with following equations:

$$\lambda = \frac{u}{V} = \frac{\omega D}{2V} \tag{10}$$

$$Cp = \frac{2Fu}{\rho V^3 DH} \tag{11}$$

$$Re = \frac{VD}{\nu} \tag{12}$$

Which V wind speed, D diameter of rotor, H height of rotor, u speed of blade's tip, ν kinematics viscosity, and ω is rotation speed of rotor.

D. Governing Equations

Equations for solving air flow field and calculating pressure and speed in different points of turbines, are conservation of mass and movement equations.

These equations in non-acceleration coordinate system for stable state are:

$$\frac{\partial}{\partial X_i}(\rho u_i) = 0 \tag{13}$$

$$\frac{\partial}{\partial X_j}(\rho u_i u_j) = -\frac{\partial p}{\partial X_i} + \frac{\partial \tau_{ij}}{\partial X_j} + \rho g_i + F_i \tag{14}$$

$$\tau_{ij} = \left[\mu \left(\frac{\partial u_i}{\partial X_j} + \frac{\partial u_j}{\partial X_i} \right) \right] - \frac{2}{3} \mu \frac{\partial u_l}{\partial X_l} \delta_{ij} \tag{15}$$

Which u_i speed of airflow in specific direction and F_i to describe effect of external forces.

E. Architecture of the neural network

In this research, the architecture of the neural network model was optimized by applying different amounts (1–7) of hidden neurons. When the increase of hidden neurons did not improve the model anymore, the model with the smallest amount and maximum performance was chosen as the best model. The choice of a specific class of networks for the simulation of a non-linear and complex map depends on a variety of factors such as the accuracy desired and the prior information concerning the input–output (TSR–power factor) pairs. The most popular ANN is the feed forward multi-layer perceptron, where the neurons are arranged into an input layer, one or more hidden layers, and an output layer. Only one hidden layer was used in this study because of the proven non-linear approximation capabilities of multi-layered feed forward perceptron network for an arbitrary degree of accuracy [13].

The variation of training error with respect to the number of neurons in the hidden layer is found for rotor "I" that this result is enable to generalization to other rotors. As seen from Fig. 4, the RMSE (training error) is minimal when the number of neurons is six.

In this work, the accuracy of the modeling with respect to the correlation coefficient index (R2), standard sum error (SSE), and root mean square error (RMSE) have been presented in Table 1.

Each neuron consists of a transfer function expressing internal activation level. Output from a neuron is determined by transforming its input using a suitable transfer function. Generally, the transfer functions are sigmoidal function, hyperbolic tangent and linear function, of which the most widely used for non-linear relationship is the sigmoidal function [14, 15]. The general form of this function is given as follows:

$$y_J = f(x_J) = \frac{1}{1 + e^{-x_J}} \tag{16}$$

This sigmoid function maps input into output in a range between 0 and 1, distributed as an S-shaped curve, so the input and output data should be scaled to the same range as the transfer function used. The software used for the ANNs modeling was Matlab Toolbox version 7.0.

IV. RESULTS AND DISCUSSIONS

Power factor (power ratio) for rotors "I" to "IV" in Reynolds number 1.5×10^5 by tip speed of blade (results of first experiment) are presented in Figures 5 and 6. According to results, each rotor might have an effective result in specific range of blade's tip speed in proportion of other rotors. For example, rotors "IV" and "V" have greater power factor then rotor "I" in low and high speed of blade's tip. But in average speed, rotor "I" has greater power factor.

In order to compare rotors and chose the best rotor curve, average power factor or total power factor is useful. In Fig. 7 total power factor is presented. Rotor "II" as the most effective rotor in different speeds of blade's tip could be seen in the Fig. 7. Rotors "VI" and "III" also have good efficiency. Because the only difference between rotors "I" to "V" is the gap distance (S) between blades, the comparison between power factor of these rotors proves that increasing distance S in rotor "II" (S =3.2 cm) in proportion with rotor "I" (S =0), causes suddenly increase in power factor and intense decrease in resistance force against rotor movement. But this increase in rotors "III" (S =3.8cm) to rotor "V" (S =7.2 cm) causes decrease in power factor.

Therefore, the best gap distance (S) is in range 0 to 3.2 cm. Besides, power factor is at maximum level when linear speed

of blade's rim is close to wind speed $(\lambda = 1)$.

The effect of gap distance (S) on power ratio could be examined by drawing speed vectors round the rotors. It is presented in results of numeric simulation. Power ratios in rotors "I" and "IV" in different Reynolds number are presented in Figures 8 and 9. According to figures, increasing Reynolds number (wind speed) leads to increase of power factor. The reason is increase of wind energy. This increase is at maximum level when $\lambda = 1$. Getting away from this maximum point means decrease of power ratio.

Average power factor for rotors "I', "II" and "IV" is compared in Fig. 10. According to the figure, increasing Reynolds number (wind speed) leads to increase in rotor's power factor. But the rate of this increase is decreasing. The reason is change in flow status and turbulence flow round the blades.

Torque on turbine's blades in different wind speed and different angles of blade in proportion of wind speed which is simulated by ANN, is presented in figures 11 to 14. According to figures, increasing wind speed leads to increase of torque. For all examined rotors, maximum amount of torque happens in angle about 60° and minimum amount of torque happens in angle about 120°. Besides, in rotor "I" area of minimum torque is vast, however for other rotors it is not in this case.

The chart of torque on different blades in wind speed 12 m/s is presented in Fig. 15. Comparing different charts proves that, although rotor "I" has the greatest torque in angles 0o to 60°, in angles greater then 60° there is serious decrease in torque. This decrease continues until angle 160°. Totally, for a complete rotation, rotor "II" has the greatest outlet torque. Relation between outlet torque of rotor and square of wind speed (or relation between power ratio and third exponent of wind speed) is presented in Fig. 16. This chart is similar for different rotors.

V. CONCLUSION

In this paper, an ANN approach is presented to estimation of power factor and torque in wind turbine. Because of the capabilities of parallel information processing and generalization of the ANNs, the proposed algorithm is found to be fast and accurate. Results prove that curves for rotors "II" to "IV" have greater power factor than other rotors, because of the gap distance between blades. On the other hand, excess increase of gap distance, leads to decrease of power factor. In this research, the best ratio is defined as $\frac{S}{D} = 0.2$. Besides, according to results of numeric solution and experiments, the best blade's curve is the curve of rotor "II". Other results prove that, increase of wind speed (Reynolds number) leads to serious increase of output power (is related to third exponent of speed).

ACKNOWLEDGMENT

ABBREVIATIONS AND SYMBOLS

A	swept area of the rotor, πR^2
Cp	power factor
D	diameter of rotor, m
H	height of rotor, m
F_i	effect of external forces
$\overset{o}{m}$	air mass flow rate, kg/s
N	number of data.
P_w	power, watt
R^2	correlation coefficient index
Re	Reynolds number
RMSE	root mean square error
SSE	standard sum error
S	gap distance, m
T	torque of vertical force to blade's surface, N.m
TSR	tip speed ratio
u	speed of blade's tip, m/s
u_i	speed of airflow in specific direction, m/s
V	wind speed, m/s
$w_{ij}(n)$	weight in nth step
$w_{ij}(n+1)$	weight of i to j element in (n+1)th step
x_{obs}	experimental values
x_{est}	estimated values
ν	kinematics viscosity, Kg/m.s

ω	rotation speed, rad/s
λ	tip speed ratio
θ	angular position of turbine
ρ	density, kg/m^3
α	momentum coefficient
η	learning rate
$\delta_i(n)$	local error

J. Sargolzaei was born in 1971 in Iran. I was studied in chemical engineering at Sistan and Baluchestan University. My researching was in soft computing. I earned my PH.D. in 2006 from Sistan and Baluchestan, Zahedan, Iran.
My researching was continued in modeling and simulation with artificial intelligent system and fuzzy system and hybrid. Also I was applied membrane system for milk ultrafiltration and it was simulated with simulink of Matlab.
A. Kianifar was born in 1955 in Iran. I was studied in Mechanical engineering at Glasgow UK in 1988. I was researched in renewable energy in strathclyde Glasgow UK.

REFERENCES

[1] Bhatti T.S. and Kothari D.P. Aspects of Technological Development of Wind Turbines, J. Energy Engineering, Vol. 129, Issue 3,2003, pp. 81-95.

[2] Gourieres D.L. Wind power plants, Pergamon Press, Oxford, England, 1982.

[3] Menet J.-L. A double-step Savonius rotor for local production of electricity: a design study, Journal of Renewable Energy, Vol. 29, 2004, pp. 1843-62.

[4] Burton F.L. Water and Wastewater Industries: Characteristics and Energy Management Opportunities, (Burton Engineering) Los Altos, CA, Report CR-106941, Electric Power Research Institute Report, p. ES-1, 1996.

[5] Savonius SJ. The Savovius rotor and its applications, Mechanical Engineering, Vol. 35(5), 1931, pp. 333-7.

[6] Testuya Kawamura, Tsutomu and Hayashi, Kazuko Miyashita Application of the domain decomposition method to flow around the Savonius rotor, 12th International Conference on Domain Decomposition Methods, 1998, Chiba, Japan.

[7] Sargolzaei J., Saghatroleslami N., Khoshnoodi M., Mosavi M. Comparative Study of Artificial Neural Nets (ANN) and Statistical Methods for Predicting the Performance of Ultrafiltration Process in the Milk Industry, Iran. J. Chem. Chem. Eng., Vol. 25, No. 2, 2006, pp. 67-76.

[8] Kalogirou S.A. Applications of neural networks for energy systems, Renewable energy, Vol. 30 (7), 2005, pp. 1075-90.

[9] Kalogirou S.A. Artificial neural networks in renewable energy systems applications: a review, Renewable Sustainable Energy Review, Vol. 5 (4), 2001, pp. 373-401.

[10] Neuro Dimensions, NeuroSolutions, 2001.www.nd.com.

[11] Zupan, J., Gasteiger, J. Neural Networks in Chemistry and Drug Design, Wiley-VCH,Weinheim, 1999.

[12] Demuth, H., Beale, M. Neural Network Toolbox User's Guide, The Mathworks, Natick, 2000.

[13] Kasabov, N.K. Foundations of Neural Networks, Fuzzy Systems and Knowledge Engineering, MIT Press, Cambridge, 1998.

[14] Hagan, T.M., Demuth, H.B., Beale, M. Neural Network Design, PWS Publishing Company, USA, 1996.

[15] Menhaj M. B. Fundamentals of neural networks, Tehran: Professor Hesabi publications, Iran, 1998.
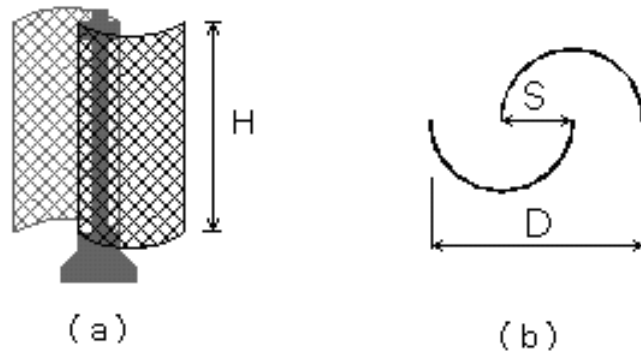
(a)   (b)

Figure 1: Schematic of a Savonius rotor. (a) Front view; (b) Semicircle shape
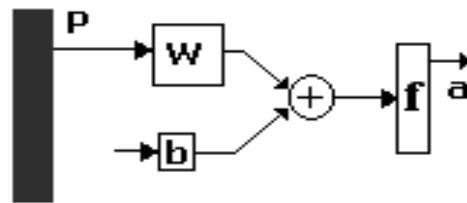

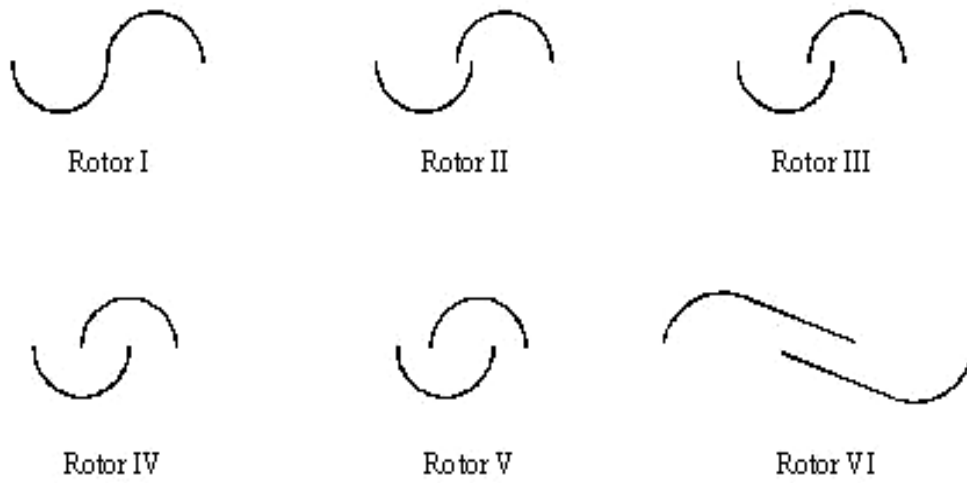Fig. 2: The architecture of the neural network

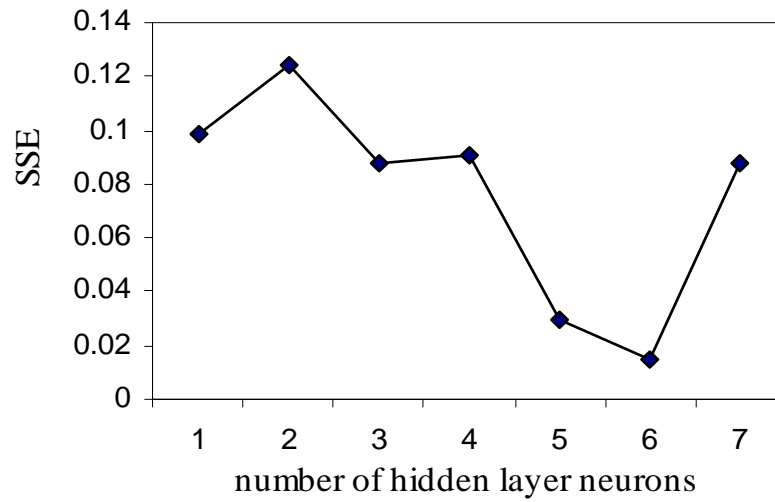Fig. 3: Shapes of experimented rotor's blades

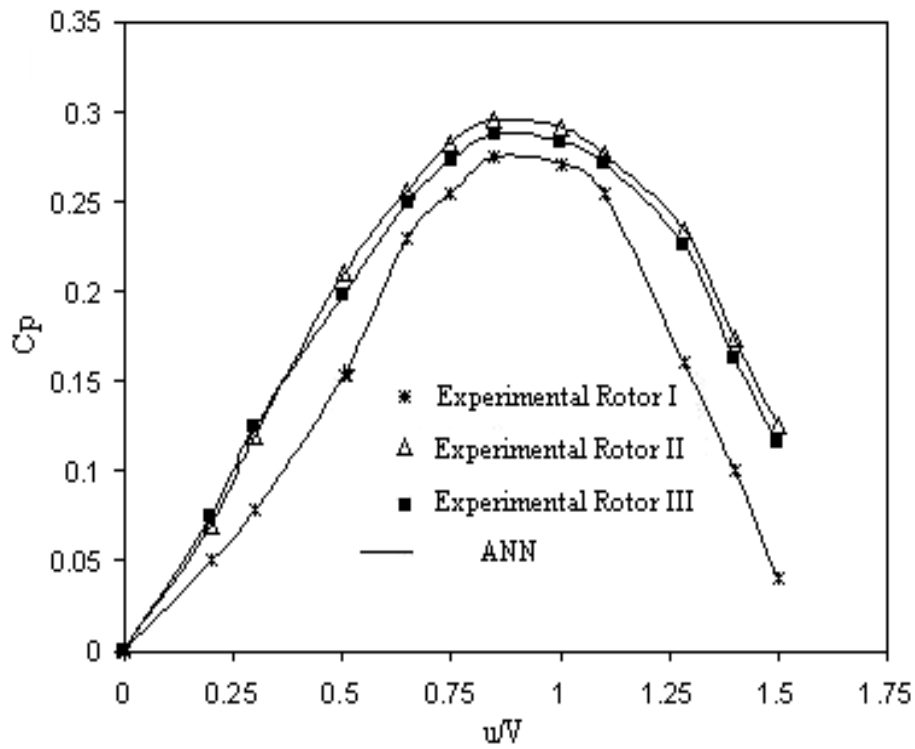Fig. 4: The effect of number of neurons in hidden layer

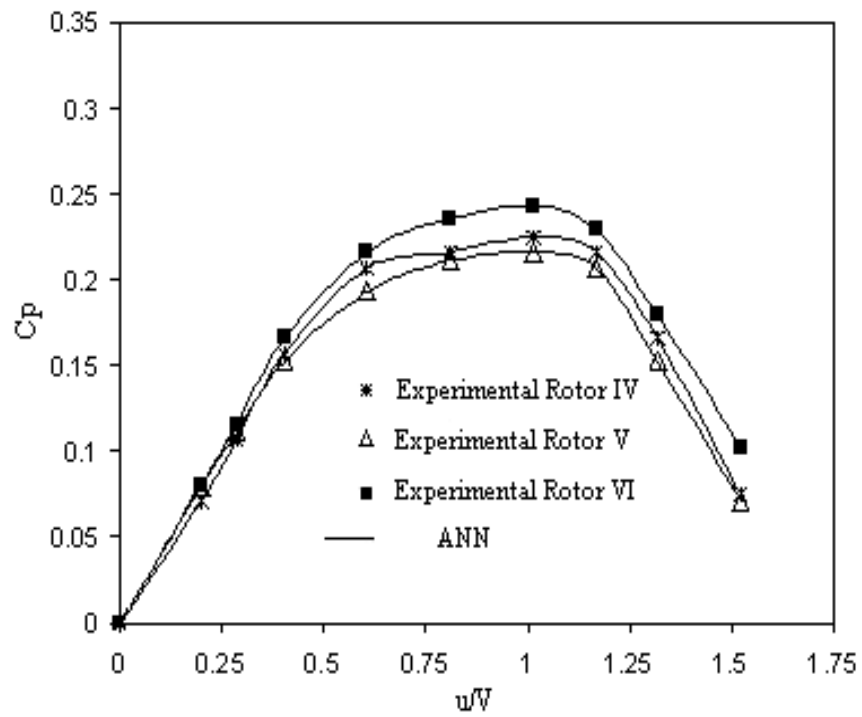Fig. 5: Comparison between power factor of rotors "I" to "III"

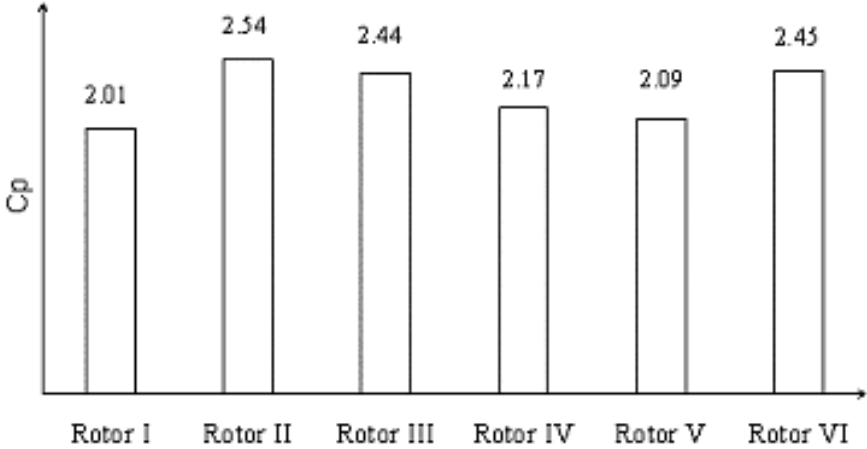Fig. 6: Comparison between power factors of rotors "IV" to "VI"

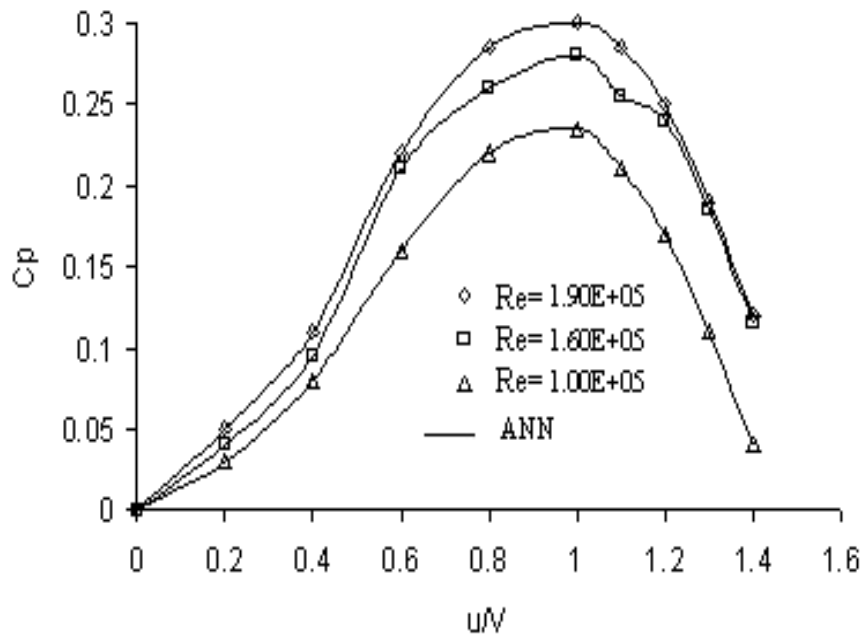Fig. 7: Comparison between power factor in rotors "I" to "VI"

Fig. 8: Rotor's power factor in different Reynolds numbers
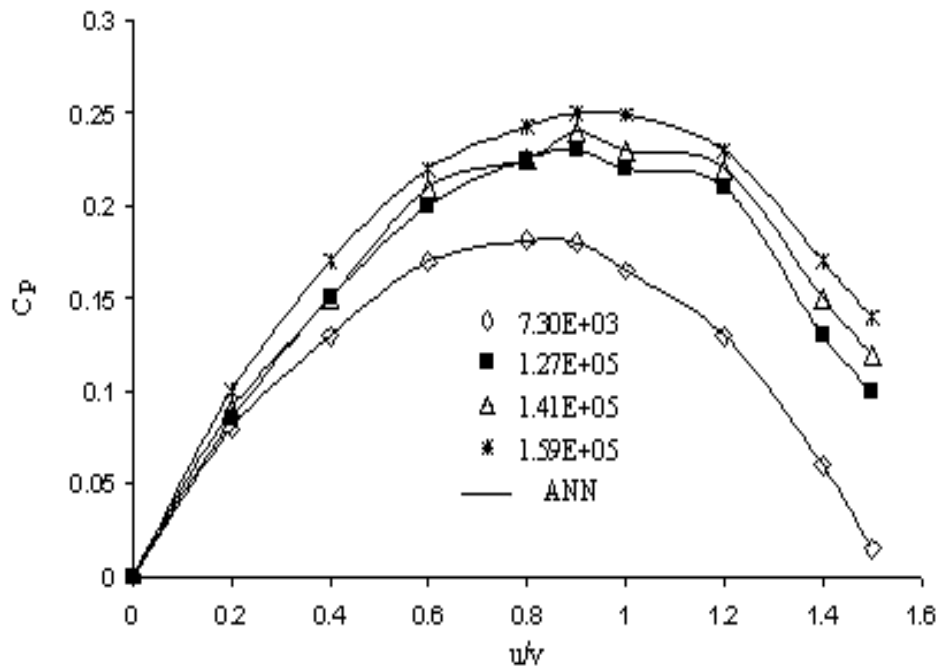
Fig. 9: Power factor in rotor "IV" in different Reynolds numbers
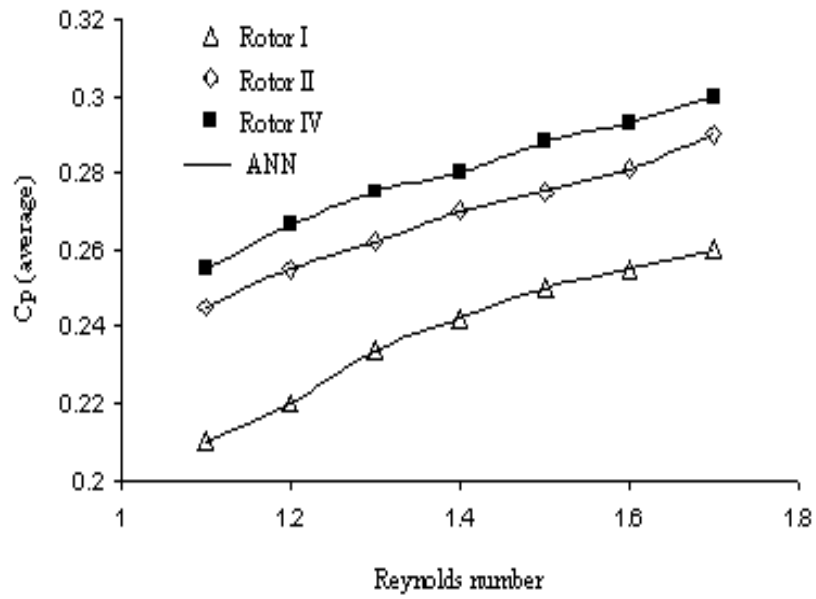
Fig. 10: Comparison of average power factor of different rotors by Reynolds numbers
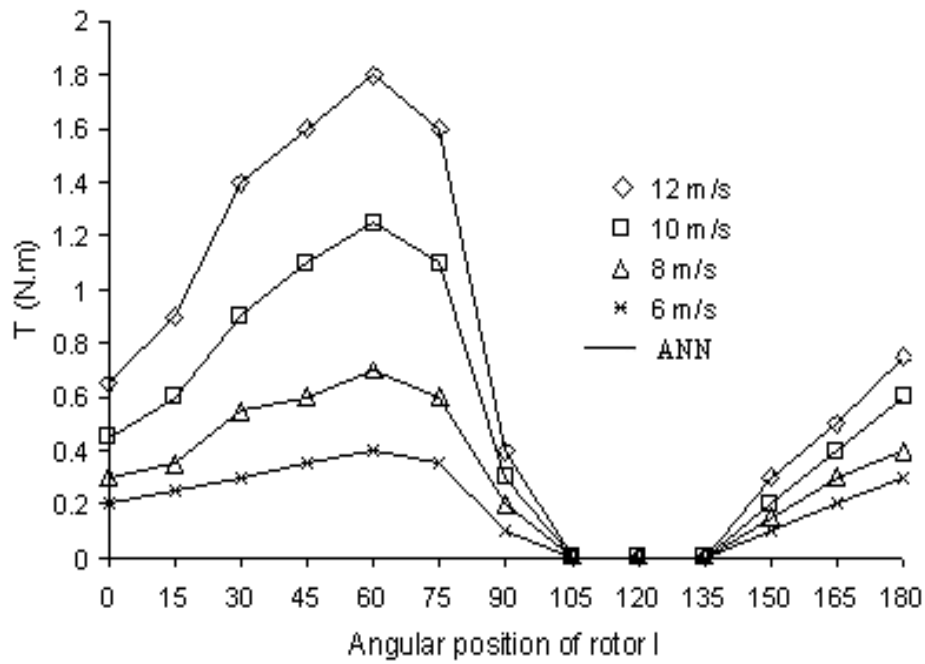
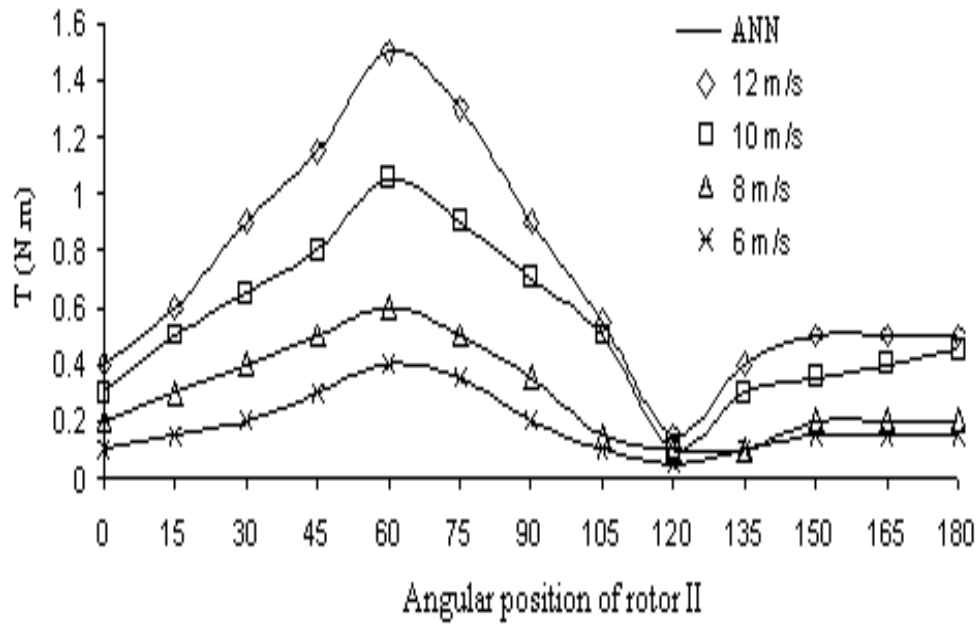Fig. 11: Torque vs. angular position of rotor "I" in different wind speeds

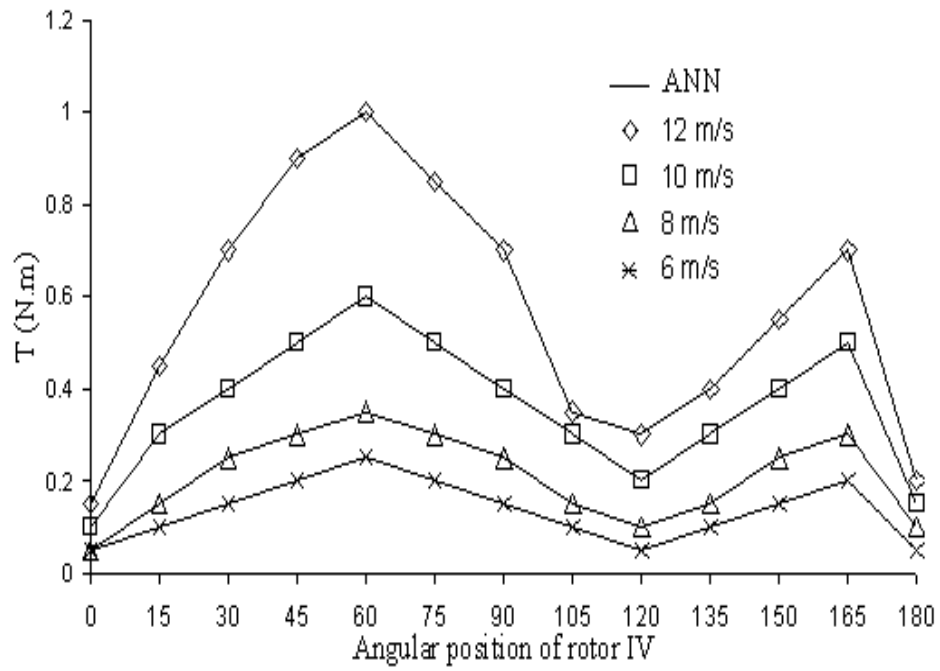Fig. 12: Torque vs. angular position of rotor "II" in different wind speeds

Fig. 13: Torque vs. angular position of rotor "IV" in different wind speeds
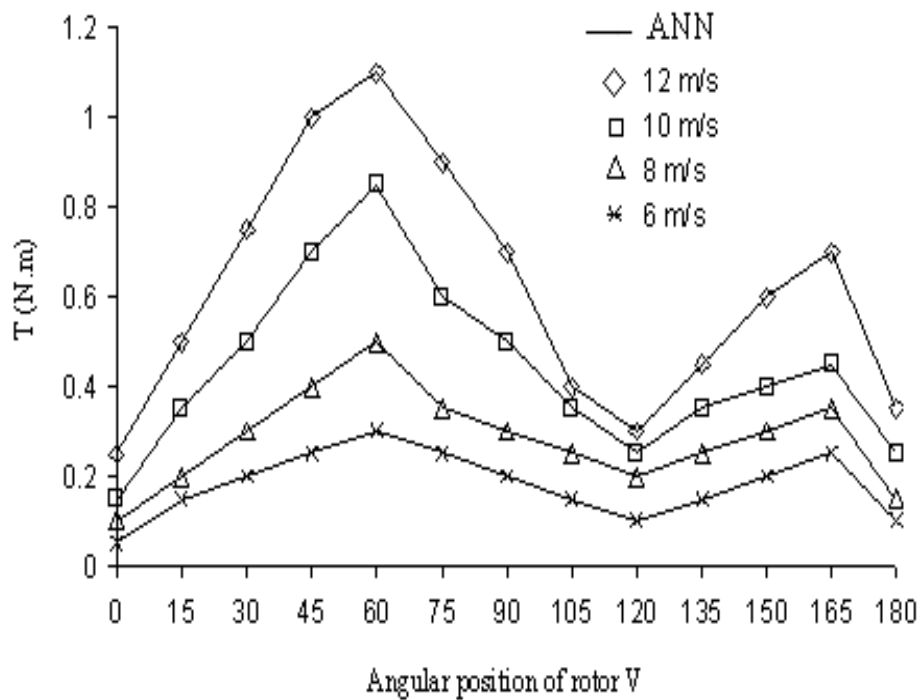
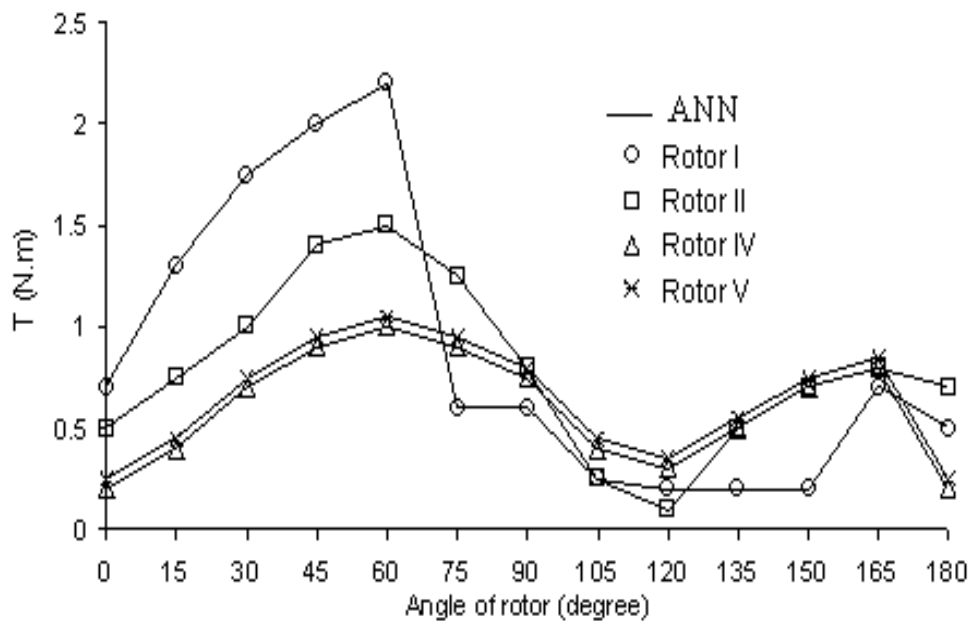Fig. 14: Torque vs. angular position of rotor "V" in different wind speeds

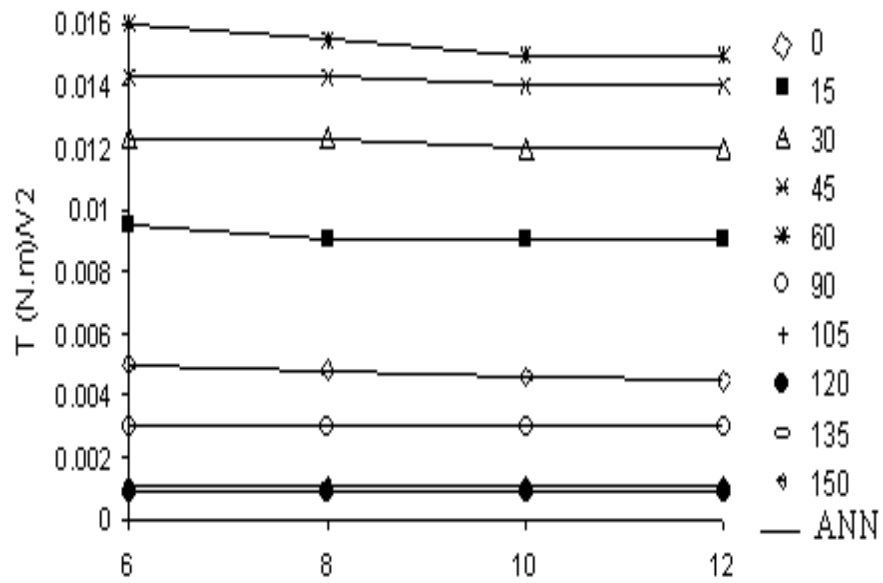Fig. 15: Comparison output torque of different rotors in wind speed 12 m/s

Fig. 16: Comparison the ratio of torque on square of speed in rotor "I"

Table 1: The accuracy of the modeling with respect to the training errors

number of hidden neuron	RMSE	R^2	SSE
1	0.01835	0.96	0.099
2	0.02056	0.95	0.1243
3	0.0172	0.965	0.0875
4	0.01761	0.9658	0.09119
5	0.01007	0.987	0.02976
6	0.0071	0.993	0.01519
7	0.0173	0.967	0.0876

Figure 1: Schematic of a Savonius rotor. (a) Front view; (b) Semicircle shape

Figure 2: The architecture of the neural network

Figure 3: Shapes of experimented rotor's blades

Figure 4: The effect of number of neurons in hidden layer

Figure 5: Comparison between power factor of rotors "I" to "III"

Figure 6: Comparison between power factors of rotors "IV" to "VI"

Figure 7: Comparison between power factor in rotors "I" to "VI"

Figure 8: Rotor's power factor in different Reynolds numbers

Figure 9: Power factor in rotor "IV" in different Reynolds numbers

Figure 10: Comparison of average power factor of different rotors by Reynolds numbers

Figure 11: Torque vs. angular position of rotor "I" in different wind speeds

Figure 12: Torque vs. angular position of rotor "II" in different wind speeds

Figure 13: Torque vs. angular position of rotor "IV" in different wind speeds

Figure 14: Torque vs. angular position of rotor "V" in different wind speeds

Figure 15: Comparison output torque of different rotors in wind speed 12 m/s

Figure 16: Comparison the ratio of torque on square of speed in rotor "I"

Table 1: The accuracy of the modeling with respect to the training errors